

A General Model for Disease Progress with Functions for Variable Latency and Lesion Expansion on Growing Host Plants

R. D. Berger and J. W. Jones

Departments of Plant Pathology and Agricultural Engineering, respectively, University of Florida, Gainesville 32611.
Florida Agricultural Experiment Station Journal Series Paper 5649.

Appreciation is expressed to T. Davoli for preparation of the figures.

Accepted for publication 21 January 1985.

ABSTRACT

Berger, R. D., and Jones, J. W. 1985. A general model for disease progress with functions for variable latency and lesion expansion on growing host plants. *Phytopathology* 75:792-797.

A disease-progress model was derived by combining an infection model with a host-growth model. Variants of common growth functions (e.g., the logistic, Gompertz, and exponential) were used as the basic equations to calculate infections and host growth in time. The model contained a feedback mechanism to limit host growth as increased disease. Variable latency was achieved by a distributed-delay submodel. The duration and shape of the latency curve could be altered by changing the number of stages in the submodel and by varying the development rates between stages. As in natural pathosystems, the simulated epidemic rates were faster at lower initial amounts of disease. The epidemic rate after an epidemic interruption was about twofold faster than the average rate. The increases in epidemic

rate could be explained solely by the amount and proportion of healthy tissue rather than by a change in any variable related to the pathogen. The rate and shape of the plant-growth curve affected the rate and shape of the disease-progress curve. Under some conditions, the areas of healthy and diseased tissue could be increasing at exponential rates but the epidemic rate was about zero; i.e., the proportion of disease did not change. If the rates of infection and host growth for a pathosystem are set as functions of environmental parameters, then the general model might be used for real-time simulation. The model may have benefit for decision-making in disease management and to estimate potential crop loss.

Various growth equations (such as the logistic, Gompertz, Richards, and Weibull) have been used to characterize the progress of disease in time (1,5,14,21). Curves for one or more of the functions usually approximate the actual progress curve. However, these simple growth equations lack substantial biological realism as models for disease progress in that several important epidemiological factors are neglected or not characterized (e.g., host growth, length of latent period, variable latency of infections, and lesion expansion).

The host growth that occurs during the epidemic may influence the rate of disease increase and the shape of the disease-progress curve (3,13). When the simple growth equations (as above) are used to describe disease progress, the influence of host growth on disease is not specifically considered. The resultant curve is a summary of disease progress as modified by the ongoing host growth. Host growth during the epidemic also causes problems in the estimation of disease (4) and the calculation of epidemic rates unless the disease proportions are appropriately transformed (21).

Okuno (as cited by Kato [12]) combined a logistic equation for disease increase with a logistic equation for host growth. With Okuno's model, Kato (12) found that, even though the rate of disease development was held constant, the epidemic rate increased as the rate of development of leaf area increased. Also, negative rates of epidemic development occurred when the increase of the diseased area was slower than the growth rate of the host. However, Kato (12) did not consider the influence of disease on host growth and compensation for latent period and lesion expansion was not incorporated into the model. Rouse (17) also suggested that host growth be incorporated into the logistic disease model. However, he also did not consider the latent period in his model and the intricacies of his general host growth variable (K) were not explored.

The effects of variable latent periods on natural disease progress are complex. Variable latency will slow the rate and smooth the

curves of disease progress and extend infections in time (20). When a population of infections occurs on a given day, t_n , the lesions that develop therefrom do not all appear on the same day one latent period (p) later at $t_n + p$. The appearance of lesions from synchronous infections are distributed as unique populations beginning at time $t_n + p$. The lesions or diseased individuals may continue to appear over several days (6), weeks (8), or months (7), depending on the pathosystem. If the population of appearing lesions is plotted, the curve may be linear (6), monomolecular (6), sigmoidal (6,18), or of another shape. To analyze the variable appearance of rust pustules on wheat after a single inoculation, Shaner (18) used the probit transformation to linearize the latency curve and to calculate a median latent period (LP_{50}).

Lesion expansion over time is also a significant component of disease progress. For many diseases, such as *Alternaria* and *Cercospora* leafspots and *Phytophthora* and *Botrytis* blights, the lesions continue to expand and affect neighboring tissue. For northern leaf blight caused in corn by *Helminthosporium turcicum*, the lesion expansion can be considerable (2).

Because of the problems and limitations noted above for current epidemiological models, a new model was developed to describe the progress of disease as influenced by host growth with special functions for variable latency and lesion expansion.

THE MODEL

Host growth. The logistic and Richards equations have been used frequently to describe host growth (10). Since the logistic equation is a common model with some flexibility, we used this equation to obtain the increase of leaf area over time. The daily increase of leaf area (dL/dt) in simulations without disease was calculated as:

$$dL/dt = k_L L(1 - L/L_{max}) \quad (1)$$

in which k_L is the rate of leaf-area increase, L is the present total leaf area, and L_{max} is the maximum leaf area. The total leaf area was accumulated over time beginning at initial leaf area (L_0) by using rectangular integration. For many of our simulations, the values were $L_0 = 1 \text{ cm}^2$, $L_{max} = 4,600 \text{ cm}^2$, and $k_L = 0.27$. These values

The publication costs of this article were defrayed in part by page charge payment. This article must therefore be hereby marked "advertisement" in accordance with 18 U.S.C. § 1734 solely to indicate this fact.

were estimated from the logistic increase in the leaf area of a sweet corn plant in which L_{max} was reached in 65 days (2). Additional host-growth curves were obtained by adjusting L_0 , k_L , and L_{max} of the logistic and other functions.

The assumption was made that the increasing disease would slow subsequent host growth because this is typical of natural pathosystems (13). A feedback function for the influence of disease severity (y) on host growth was then necessary. The daily increase of leaf area per plant in the presence of disease was:

$$dL/dt = k_L L (1 - y) (1 - L/L_{max}) \quad (2)$$

in which $(1 - y)$ represents the fraction of disease-free leaf area to provide the necessary feedback on host growth. The total leaf area (L) in the presence of disease was accumulated as above.

Disease increase. The logistic equation has also been used frequently to characterize disease progress (1,5,14,21). The logistic equation for the rate of disease increase is:

$$dy/dt = r y (1 - y) \quad (3)$$

in which dy/dt is the daily increase in disease proportion y , and r is the apparent infection rate (21). In the simple logistic rate equation (equation 3), the latent period is not specifically considered so an alternative form was desired. In equation 3, disease begets disease rather than the biologically more correct: disease begets infection that leads to disease after time p . Consequently, the daily increase of infected leaf area (dI/dt) was derived in the new model as:

$$dI/dt = k_Y Y (1 - I/L) \quad (4)$$

in which k_Y is a true infection rate based on area of diseased tissue, rather than an apparent rate derived from the proportion of visible disease, and Y is the present total diseased leaf area (not disease proportion). The modified logistic-infection equation (equation 4) can be interpreted as: the present diseased area (Y) leads to daily infection (dI/dt) by infection rate (k_Y) and is limited by the proportion of healthy tissue remaining to be infected ($1 - I/L$). The daily increase in infected leaf area was integrated over time, beginning with initial infected (not diseased) leaf area (I_0).

The daily diseased leaf area (dY/dt) that appeared one latent period later was calculated as a pure delay function:

$$dY/dt = dI(t - p)/dt \quad (5)$$

in which p is the latent period. The daily diseased area was integrated over time beginning from the initial diseased area (Y_0). In simulations, $I_0 > Y_0$ and both parameters were varied to study the influence of initial infected and diseased areas on disease progress.

The proportion disease (y) was calculated from the total diseased area (Y) and the total leaf area (L) for any time (t) as:

$$y = Y/L \quad (6)$$

To compare simulated epidemics with the various models and parameters, the progress curves were either plotted versus time in linear-linear scale or else the disease proportions were first transformed into logits ($\log_e(y/(1 - y))$). An average epidemic rate (r) was calculated as: $r = (\text{logit}(y_2) - \text{logit}(y_1))/(t_2 - t_1)$ (5,21), in which t_1 and t_2 were selected for points of interest along the curve.

Variable latency. In equation 5, all synchronous infections (dI/dt) at time t_n from equation 4 would appear as lesions (dY/dt) in a single step at time $t_n + p$. Since variable latency is the general rule for known pathosystems (18; and 21, pages 68-69), an alternative submodel for the differential appearance of lesions in time was sought. In pest modeling, several approaches have been used to handle age or stage structure problems (15,22). The various ages of infections could be handled in matrices or as eigenvalues and eigenvectors. Both procedures are sometimes difficult to handle and interpret. The matrix approach results in a waste of computation time and storage because the matrices are comprised

mostly of zeros. An alternative and seemingly preferential approach (15,22) is to use a distributed-delay function to generate a distribution of stage-completion times. In its simplest form, the infections would flow through a series of substages (a) and emerge as a distribution of developing times described by the gamma (Erlang) function. If there is one substage ($a = 1$), the distribution of appearing infections would be a negative exponential. If $a > 5$, the distribution approaches a normal curve (Fig. 1). Thus, the distributed-delay function is a very versatile function for the modeling of variable stage-completion times. The time of appearance of the first lesion (p_0) and last lesion (p_{max}), the duration ($p_{max} - p_0$), the LP_{50} , and the shape of the curve for variable latency of various pathosystems can be closely approximated by adjusting the number of substages and the development rates (k_D) between them. For our simulations, the development rates between substages were held equal; i.e., $k_{D1} = k_{D2} = k_{D3} = \dots k_{Dn}$. As one example, if $a = 2$ and $k_D = 0.95$, then 95% of all lesions of synchronous infections would appear within five days of p_0 in a near-monomolecular fashion.

Lesion expansion. For some pathosystems, the rate of lesion expansion is primarily a function of ambient temperature and tends to be linear over time (2). The lesion expansion in the disease-progress model was handled as a simple additive function to equation 5:

$$dY/dt = dI(t - p) / dt + X Y \quad (7)$$

in which X is the rate of lesion expansion per unit of diseased area.

The general model is represented by equations for dL/dt , dI/dt , dY/dt , and y . These equations were solved by computer simulation using the CSMP programming language (11) with the rectangular integration option. The source code for the model in CSMP is given in Fig. 2; this particular example has four substages for infections in the distributed-delay function to achieve variable latency. An integration time step (Δt) of 0.05 days was used. The simulations were run on an IBM 3081 computer in the Northeast Regional Data Center at the University of Florida, Gainesville. An alternate program of the model was written in BASIC language for microcomputers.

SIMULATION RESULTS

Host growth. The host-growth curves generated by the logistic function in the combined host-growth/disease model were

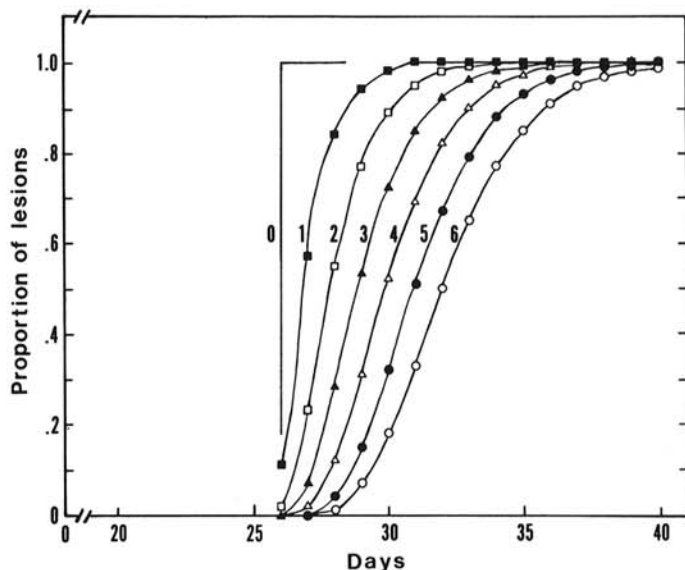


Fig. 1. The variable appearance of lesions over time from synchronous infection on day 20 and a minimum latent period of 6 days. The curves for variable latency were obtained with zero to six substages in a distributed-delay function. With zero substages, all lesions appeared on day 26; with six substages, lesions continued to appear over more than 13 days.

sigmoidal regardless of the intensity of disease or the model chosen for the disease progress. To simulate a nearly mature crop, an initial high leaf area ($L_0 = 4,550 \text{ cm}^2$) and slow growth rate ($k_L = 0.01$) were used. Intermediate values for these parameters were also tested. When growth rate (k_L) was increased, the growth curves remained sigmoidal but the maximum leaf area (L_{\max}) was reached earlier.

In addition to the logistic equation, several other functions for host growth were examined. The derivatives of these functions were substituted for equation 2 in the combined model: linear ($dL/dt = k_L(1-y)$, $k_L = 60$); exponential ($dL/dt = L_0 k_L \exp(k_L t)$ ($1-y$), $k_L = 0.033$); or Gompertz ($dL/dt = k_L L (-\log_e(L/L_{\max}))$ ($1-y$), $k_L = 0.07$). The generated host-growth curves with these latter equations were typical for the respective function.

Host growth and disease. Simulated disease progress was sigmoidal when the modified logistic equation was used as the infection model. The average epidemic rate (r) generally increased with each increase in the rate (k_L) of host growth, even though k_Y was constant. However, when initial leaf area was high ($L_0 > 100 \text{ cm}^2$) or growth rate was very fast ($k_L > 0.35$), most of the host growth occurred while $y < 0.01$. Consequently, increases in either initial host area or host growth rate above these aforementioned values had no noticeable effect on the epidemic rate. The rate of host growth had an effect on epidemic rate only when considerable host growth occurred at $y > 0.01$.

When generated host growth was slowed ($k_L = 0.01$) for 10 days during the epidemic (e.g., when $y = 0.2$ and $r = 0.1$) and the epidemic was allowed to proceed at a constant infection rate ($k_Y = 2$), the average epidemic rate quickly became more rapid ($r = 0.25$) in the period in which host growth was slow. This rapid increase in simulated disease occurred with both variable and fixed

latent periods and resulted in the earlier occurrence of high disease intensity that subsequently limited total host growth.

The simulated disease-progress curves with the logistic-infection model were also sigmoidal when host growth was generated with either the linear or Gompertz functions. For both host-growth functions, the $(1-y)$ feedback mechanism caused a gradual slowing of host growth that reached an asymptote of L_{\max} lower than without the feedback. With the exponential host growth function, early disease progress was sigmoidal but the disease progress reached an asymptote at $y < 1$. The asymptotic level was dependent on the rates k_Y and k_L and occurred when the daily infected area (dI/dt) was equivalent to the daily host growth (dL/dt). With $k_L = 0.094$ and $k_Y = 2$, the asymptote was $y = 0.37$; whereas at $k_Y = 5$, the asymptote was $y = 0.41$. Even though both host area and infected area were increasing at an exponential rate ($< k_L$), the epidemic rate was virtually zero ($r = 0 \pm 0.001$) for > 30 days.

Simulations of disease progress were also made without the $(1-y)$ feedback mechanism on host growth. For all four plant growth functions, the disease increased sigmoidally until all available healthy host area was infected. Thereafter, the disease-progress curves mimicked the host-growth curve in shape and rate.

Reduction in initial disease. If host growth was increasing when $y > 0.01$, then the epidemic rate (r) increased with each reduction in initial infected (I_0) and initial diseased (Y_0) areas. If most host growth occurred prior to $y \approx 0.01$, then epidemic rate was not affected by decreasing I_0 and Y_0 ; however, the time to $y = 0.5$ was delayed.

Variations in infection rate (k_Y). In equation 4, the latent period is included intrinsically because the daily infections are dependent upon the diseased area and not directly from the total infected host area. With this inclusion of the latent period in the equation, the values of infection rates (k_Y) were not in the numerical range of values usually associated with the average apparent infection rates (r) for many fungal leaf diseases ($0.1 < r < 0.6$) (21, page 216; 23, pages 166 and 326). The values of k_Y for epidemics of most leaf diseases are expected to be in the range $0 < k_Y < 20$. The calculated epidemic rates for the period between $y_1 = 0.01$ to $y_2 = 0.9$ ranged from $r = 0.15$ for simulations with $k_Y = 0.5$ to $r = 0.425$ for $k_Y = 10$.

Epidemic interruption. In some simulations, the infections were halted ($k_Y = 0$) in certain time periods to mimic the effect of unfavorable weather for disease or the application of a control procedure. This interruption in infection resulted in an interruption of disease, offset in time by one latent period. When this interruption of infection occurred during ongoing host growth, the epidemic rate after the interruption was about twofold faster than the average rate prior to the interruption (Fig. 3). A faster rate after an epidemic interruption has been frequently observed in natural pathosystems (3). The increasing host growth during the interruption diluted the diseased area and resulted in a negative epidemic rate. The epidemic rates during the interruptions became less negative as the values of y at the time of the interruption were higher. If host growth was slow (e.g., $k_L = 0.01$) during the interruption, the epidemic rate was positive but slow. After the interruption, the epidemic rate was faster than before the interruption (Fig. 4), but was less than when host growth was substantial. The rapidity of change in epidemic rate from average to slow to fast during these epidemic interruptions was dependent upon the parameters of variable latency. If the latency was not variable ($a = 0$, and e.g., p_0 , LP_{50} , and $p_{\max} = 9$), the epidemic rates changed abruptly, and were displaced in time from the interruption by one latent period (Fig. 5). With variable latency (e.g., $a = 4$, $p_0 = 5$, $LP_{50} = 9$, and $p_{\max} = 17$), the changes in rate following the interruption were gradual swings because of the late- and early-appearing lesions (Figs. 3-5). Additional infections would contribute to slightly higher epidemic rates if $k_Y > 0$ during the interruption.

Other disease-progress models. Although the logistic equation is commonly used to model disease progress, the curves generated by this equation do not always depict the natural disease progress in early epidemic stages (5). Consequently, other disease-progress

TITLE DISEASE PROGRESS MODEL WITH TITLE DISTRIBUTED DELAY

```
MEMORY LOGIT2
MEMORY A1DOT
INITIAL
PARAM L0=1.
PARAM LMAX=4600.
PARAM INFO=1.0E-1
PARAM Y0=1.0E-2
PARAM KL=.27
PARAM KY=2.
PARAM KD=.95
PARAM P=5.
PARAM LX=0.
DYNAMIC
LDOT=KL*LA*(1.-Y)*(1.-LA/LMAX)
INFDOT=KY*YA*(1.-TINFA/LA)
TINFA=INTGRL(INFO,INFDOT)
LA=INTGRL(L0,LDOT)
A1DOT=DELAY(10,P,INFDOT)
A2DOT=KD*A1
A3DOT=KD*A2
A4DOT=KD*A3
A5DOT=KD*A4
A1=INTGRL(0.,A1DOT-A2DOT)
A2=INTGRL(0.,A2DOT-A3DOT)
A3=INTGRL(0.,A3DOT-A4DOT)
A4=INTGRL(0.,A4DOT-A5DOT)
YA=INTGRL(Y0,A5DOT+LX*YA)
Y=YA/LA
YDIS=LIMIT(.0001,.9999,Y)
LOGIT=ALOG(YDIS/(1.-YDIS))
LOGIT2=DELAY(10,2.,LOGIT)
VDPR=(LOGIT-LOGIT2)/2.
TERMINAL
TIMER FINTIM=90.,OUTDEL=1.,DEL T=.05
PRTPLOT Y(0.,1.,LA,YA,A5DOT)
PRTPLOT LOGIT(-6.,5.,VDPR,A1DOT,TINFA)
PRTPLOT LA(0.,4600.,L0DOT,INFDOT)
END
```

Fig. 2. CSMP source code for the disease-progress model during changing host growth. In this example, four substages (A1-A4) are used in a distributed delay to achieve variable latency.

models may be more appropriate and can be substituted for the general logistic-infection model (equation 4). Some simulations were made with a modified Gompertz function in which infections were calculated as:

$$dI/dt = k_Y Y (-\log_n(I/L)) \quad (11)$$

The Gompertz-infection model provided faster disease progress than the logistic model when $y < 0.05$ (Fig. 6). When k_Y increased from 0.5 to 10 with the Gompertz model, the average epidemic rates (r) increased from 0.2 to 0.46. The response during epidemic interruption with the Gompertz model was similar to that obtained with the logistic model.

Lesion expansion. As lesion expansion increased from $X = 0$ to $X = 0.5$ (50% per day), the epidemic rates also increased (e.g., from $r = 0.2$ to $r = 0.3$). Simulated disease-progress curves were less sigmoidal and more exponential when lesion expansion was substantial (Fig. 7).

DISCUSSION

The logistic equation as used by Vanderplank (21) to describe disease progress is simple, versatile, and extremely useful to interpret epidemic rates. However, because of the simplistic nature of the model, considerable biological realism is lost. Interpretation of the curve shape and epidemic rate has often been hampered by the lack of specific information on changes in host leaf area (3). Various important epidemiological parameters are included in the new model (equations 4, 5, and 7), and the interpretation of the curves is improved.

Vanderplank (21, pages 68-69) was aware of the problem of variable latency and he provided several examples to show that the mean value of p , rather than a constant value of p , provided only a

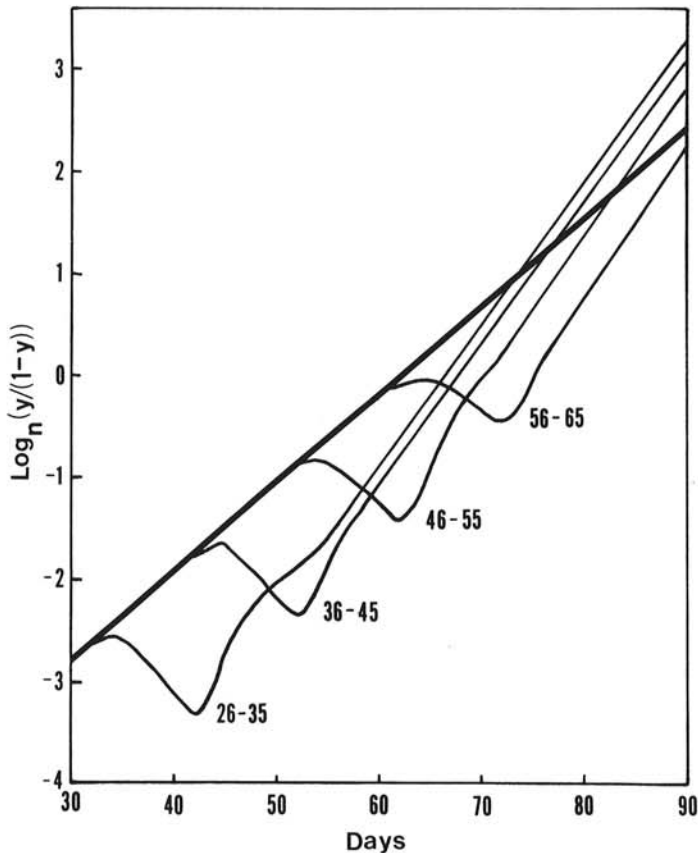


Fig. 3. Simulated disease progress (logit scale) following 10-day interruptions in infection during host growth at $k_L = 0.01$ from $L_0 = 1$. The bold line represents uninterrupted disease progress at $k_Y = 2$. The decreases in disease for 10 days after the latent periods ($p = 5$ days) occurs because of host growth.

slight error in the estimation of r . In our simulations, however, the differences in responses from a mean value of p and a constant p were substantial, both for progress of the general epidemic and for the changing rates around epidemic interruption (Figs. 5 and 6).

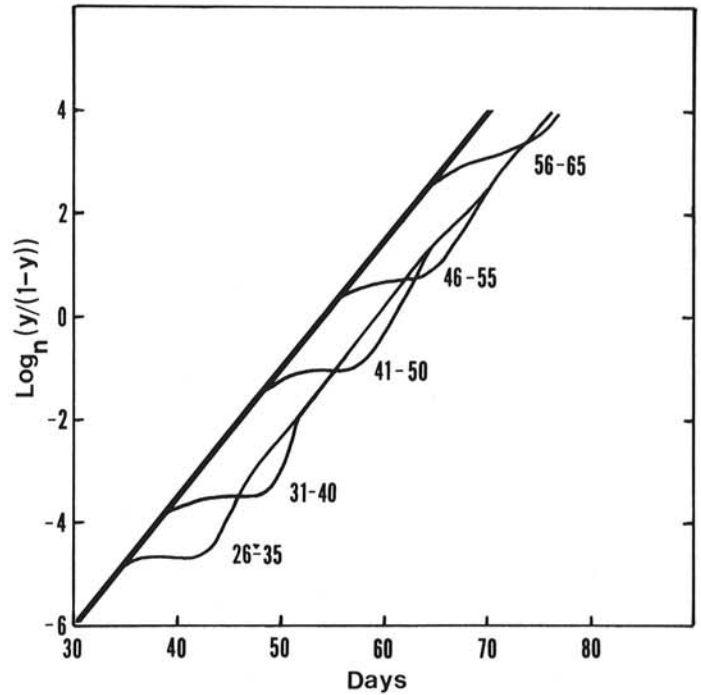


Fig. 4. Simulated disease progress (logit scale) following 10-day interruptions in infection during minimal host growth at $k_L = 0.01$ from $L_0 = 4550$. The bold line represents uninterrupted disease progress at $k_Y = 2$. The epidemic rate is faster than in Fig. 3 because host area is not limiting disease progress.

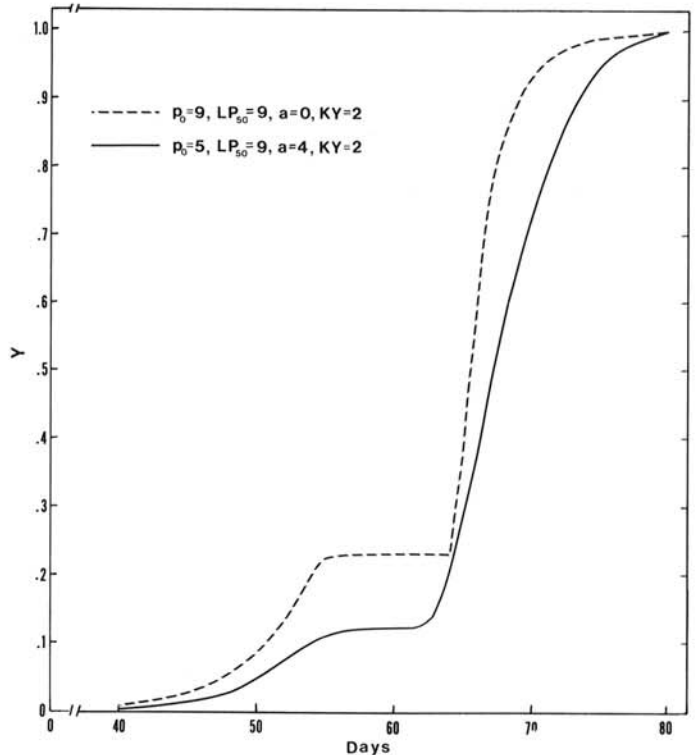


Fig. 5. Simulated disease progress following interruption in infection for 10 days for two instances of variable latency ($a = 0$ and 4). In both instances, the median appearance of lesions (LP_{50}) from synchronous infections was 9 days.

Serious errors in interpretation of disease-progress curves could result if the variable latency of infections is ignored.

Vanderplank (21, page 77) was also concerned with the effect of expanding lesions on the epidemic rate. Our lesion expansion function (equation 7) is too simplistic to represent the average growth of all lesions at all epidemic stages. In actual epidemics, the relative lesion expansion rate slows as lesions become crowded (19). It may be more satisfactory to develop a separate submodel for lesion expansion, with the submodel based on the density and ages of lesions.

The new infection model provided realistic curves of disease progress with the interaction of host growth. The model was used to aid the interpretation of previous perplexing epidemiological

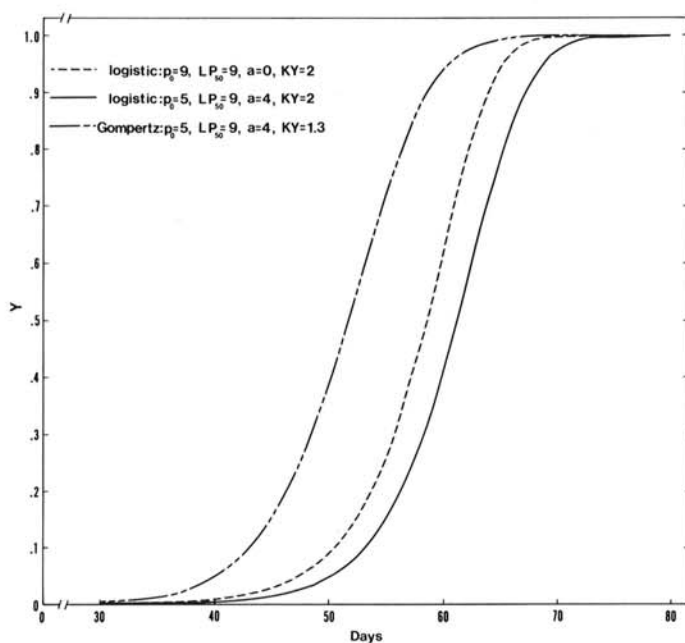


Fig. 6. Simulated disease progress for the Gompertz-infection model and the logistic-infection model with two instances of variable latency ($a = 0$ and 4). All curves began at $y_0 = 0.0001$.

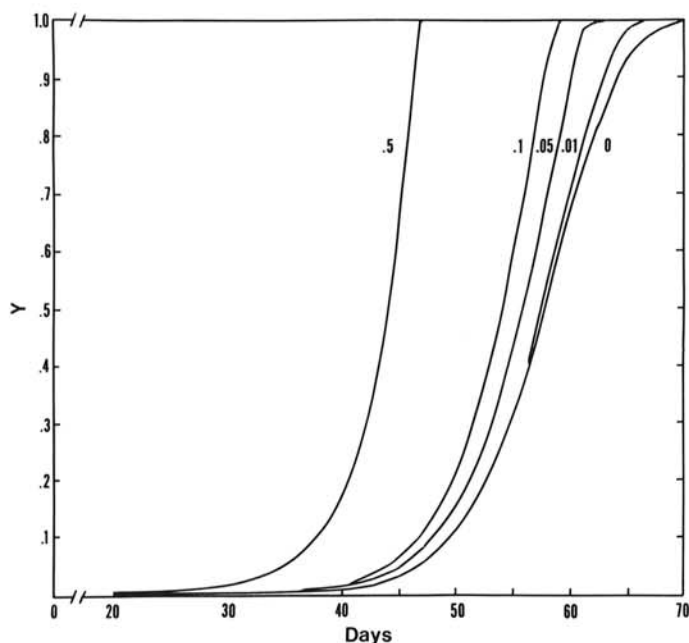


Fig. 7. Response of increasing lesion expansion (X) on simulated disease progress. Values of X are proportional increase of all diseased areas per day.

responses. The rapid disease progress following epidemic interruption was once thought to be caused by unusually large amounts of inoculum that saturated the available host tissue (23, page 224). Further, the increase of epidemic rate with the decrease in initial disease defied accurate interpretation (9, 16). With the new model, both phenomena could be interpreted solely by the amount and proportion of uninfected host area and not by any changes in parameters related to the pathogen.

We used the total leaf area (L) as being vulnerable to infection, but this is not realistic for some pathosystems. If mature tissue is resistant to infection, only the newly emerging tissue should be entered into the model. The disease-progress curves would mimic then the host-growth curve in shape and rate as has been seen in two pathosystems (1, 2).

The quantification of host growth in the disease-progress model provided substantial improvement in interpretation of the progress curves. Apparent infection rates are generally calculated from the proportion of visible disease. Serious errors could result if the interpretation of the disease-progress curve is based on these apparent rates. A rate near zero would be interpreted as very slow disease increase, when in actuality, the disease and host growth could be increasing at exponential rates. The apparent infection rates would need to be corrected for host growth either as Vanderplank suggested (21, pages 94-96), or by the simple addition of the rate of host growth to the apparent infection rate for proportions of visible disease. For example, if the host was increasing at a logistic rate of $k_L = 0.21$ and the apparent infection rate for visible disease was $r = 0.18$, then the corrected rate would be $r_c = 0.39$ ($0.21 + 0.18$).

In disease management, it is most difficult to estimate the speed and amount of disease increase following epidemic interruption. The new model should provide a reasonable estimate of this disease increase.

The infection model may have broad applicability in crop-loss determinations, because the feedback mechanism limits host growth. Disease stress in the form of reduced total host area and the intensity of disease thereon can be specifically partitioned. Decision thresholds for control application will be easier to define on the basis of the generated L and Y from the simulated epidemic. The $(1 - y)$ feedback function may be too severe or too mild a correction for some pathosystems. In the presence of disease, some hosts may respond by compensating with additional growth, other hosts may senesce earlier. Also, the implied linear relationship in the feedback of disease intensity and host growth may not be accurate over the range of $0 < y < 1$.

The combined model with its numerous mathematical variations can be the initial model to develop an epidemic simulator of any pathosystem. The researcher needs only to choose the representative functions and parameters that fit the natural host growth and disease progress. With the addition of variable latency, lesion expansion, and other submodels, the simulator could become as complex and as detailed as the researcher desires.

The growth rates k_Y and k_L as we used them in the combined model can be considered maximum rates. As the epidemic limits of various pathosystems become known, the rates k_Y and k_L can be set as a function of certain environmental parameters. The combined model could then be used to obtain real-time simulation of the selected pathosystem.

LITERATURE CITED

1. Analytis, S. 1973. Zur Methodik der Analyse von Epidemien dargestellt am Apfelschorf (*Venturia inaequalis* (Cooke) Aderh.). Acta Phytomedica. 1:1-46.
2. Berger, R. D. 1973. *Helminthosporium turcicum* lesion numbers related to numbers of trapped spores and fungicide sprays. Phytopathology 63:930-933.
3. Berger, R. D. 1977. Application of epidemiological principles to achieve plant disease control. Annu. Rev. Phytopathol. 15:165-183.
4. Berger, R. D. 1980. Measuring disease intensity. Pages 28-31 in: Proc. E. C. Stakman Commemorative Symposium on Crop Loss Assessment. University of Minnesota Misc. Publ. 7.

5. Berger, R. D. 1981. Comparison of the Gompertz and logistic equations to describe disease progress. *Phytopathology* 71:716-719.
6. Berger, R. D., and Bartz, J. A. 1982. Analysis of monocyclic pathosystems with *Erwinia-Lycopersicon* as the model. *Phytopathology* 72:365-369.
7. Dabek, A. J. 1975. The incubation period, rate of transmission, and effect on growth of coconut lethal yellowing disease in Jamaica. *Phytopathol. Z.* 84:1-9.
8. Dean, J. L. 1982. The effect of wounding and high-pressure spray inoculation on the smut reactions of sugarcane clones. *Phytopathology* 72:1023-1025.
9. Gregory, L. V., Ayers, J. E., and Nelson, R. R. 1981. Reliability of apparent infection rates in epidemiological research. *Phytopathol. Z.* 100:135-142.
10. Hunt, R. 1981. The fitted curve in plant growth studies. Pages 283-298 in: *Mathematics and Plant Physiology*. D. A. Rose and D. A. Charles-Edwards, eds. Academic Press, London.
11. IBM. 1972. *System/360 Continuous System Modeling Program User's Manual*. GH20-0367-4. 76 pp.
12. Kato, H. 1974. Epidemiology of rice blast disease. *Rev. Plant Prot. Res.* 7:1-20.
13. Kranz, J. 1975. Beziehungen zwischen Blattmasse und Befallsentwicklung bei Blattkrankheiten. *Z. Pflanzenkrankh.* 82:641-654.
14. Madden, L. V. 1980. Quantification of disease progression. *Prot. Ecol.* 2:159-176.
15. Manetsch, T. J. 1976. Time-varying distributed delays and their use in aggregative models of large systems. *IEEE Trans. Systems, Man, and Cybern.* SMC-6:547-553.
16. Plaut, J. L., and Berger, R. D. 1981. Infection rates in three pathosystem epidemics initiated with reduced disease severities. *Phytopathology* 71:917-921.
17. Rouse, D. I. 1983. Plant growth models and plant disease epidemiology. Pages 387-398 in: *Challenging Problems in Plant Health*. T. Kommedahl and P. Williams, eds. American Phytopathological Society, St. Paul, MN. 538 pp.
18. Shaner, G. 1980. Probits for analyzing latent period data in studies of slow-rusting resistance. *Phytopathology* 70:1179-1182.
19. Shaner, G. 1983. Growth of uredinia of *Puccinia recondita* in leaves of slow- and fast-rusting wheat cultivars. *Phytopathology* 73:931-935.
20. Shaner, G., and Hess, F. D. 1978. Equations for integrating components of slow leaf-rusting resistance in wheat. *Phytopathology* 68:1464-1469.
21. Vanderplank, J. E. 1963. *Plant Diseases: Epidemics and Control*. Academic Press, New York. 349 pp.
22. Welch, S. M., Croft, B. A., Brunner, J. F., and Michels, M. F. 1978. PETE: An extension phenology modeling system for management of multi-species pest complex. *Environ. Entomol.* 7:482-494.
23. Zadoks, J. C., and Schein, R. D. 1979. *Epidemiology and Plant Disease Management*. Oxford University Press, New York. 427 pp.